Soft Matter

PAPER

View Article Online
View Journal | View Issue

Cite this: *Soft Matter*, 2019, 15, 408

Phototaxis of active colloids by self-thermophoresis†

Nan Yu,[ab] Xin Lou,[b] Ke Chen*[ab] and Mingcheng Yang*[ab]

Received 12th September 2018,
Accepted 30th November 2018

DOI: 10.1039/c8sm01871e

rsc.li/soft-matter-journal

Phototaxis usually refers to the ability of a motile micoorganism to move directionally within a light gradient, which is important for microorganisms to gain energy or avoid damage. Here, we show that an active Janus particle driven by self-thermophoresis from light heating is able to exhibit significant phototactic motion by means of mesoscale dynamics simulation. Depending on the particle–fluid interactions, the active particle can move along or against the light gradient, corresponding to positive or negative phototaxis, respectively. We find that the phototaxis of the active colloid is determined by various mechanisms, including alignment (polarization) of the particle to the light gradient, orientation-dependent motility and spatially inhomogeneous motility. Our results shed light on the phototactic behavior of artificial active colloids and open up a new possibility to design photo-responsive micromachines.

I. Introduction

Phototaxis is often observed in motile microorganisms, with green algae and *Euglena gracilis* as prominent examples.[1,2] With phototactic ability, the microorganisms can swim towards a light source to receive more food or energy, or away from it to avoid radiation damage or predators. Inspired by nature, a number of synthetic micromotors have been developed to mimic their biological counterparts based on different physical and chemical effects.[3–8] Designing synthetic microswimmers that can actively sense light signals and display phototaxis would provide a versatile way for controlling their motions, which is critical for most practical applications in fluctuating fluid environments. Moreover, phototaxis also belongs to a class of fundamental nonequilibrium physical phenomena, namely the response of active colloids to external fields.[9–14]

Phototaxis of artificial active colloids has recently attracted considerable interest. In most reports, artificial active colloids are driven by light-induced chemical gradients.[15–20] The active particles employed in those studies may be roughly divided into two categories based on their structures: isotropic colloidal spheres and Janus particles. For isotropic particles, the irradiated side of the particle receives more photons under directed illumination than the shaded side due to the limited penetration depth of light.[17,19] This shading effect leads to a local light gradient across the particle in the direction of light propagation, which translates into a chemical gradient *via e.g.* a photocatalytic reaction on the particle surface. Consequently, the particle experiences self-propulsion parallel to the incident light through self-diffusiophoresis or self-electrophoresis. This may be the simplest way to achieve phototaxis, but these isotropic particles cannot properly mimic biological microswimmers as their self-propelled directions are imposed by the external field instead of inherent asymmetry. They exhibit no directed motion in a highly symmetric light field. On the other hand, Janus particles as typical microswimmers are relatively more appropriate to study phototactic behavior. Recent experiments[15,16] have shown that a Janus particle can reorient in a uniform beam or in a light gradient induced by an aligning phoretic torque due to nonsymmetric irradiation, and thereby swims phototactically.

Besides chemical gradients, light can create thermal gradients across light-absorbing particles to drive their self-thermophoretic motion.[5,21,22] However, phototaxis based on self-thermophoresis has been rarely reported. A recent theoretical study indicates that an isotropic light-absorbing particle can drift self-thermophoretically toward the light source due to the shading effect.[23] In addition, a Janus particle partly coated with light-absorbing material is theoretically shown to orient to the beam intensity gradient due to a thermophoretic torque,[12] suggesting possible phototactic motion of such Janus particles. Overall, in existing work on the phototaxis of active Janus colloids, the alignment effect (polarization) is assumed as the underlying mechanism of the phototaxis. However, other possible mechanisms need to be considered too. Even in the absence of alignment, inhomogeneous illumination may lead to orientation- and position-dependent motility of a Janus particle and hence biases

[a] *Beijing National Laboratory for Condensed Matter Physics and CAS Key Laboratory of Soft Matter Physics, Institute of Physics, Chinese Academy of Sciences, Beijing 100190, China. E-mail: kechen@iphy.ac.cn, mcyang@iphy.ac.cn*
[b] *School of Physical Sciences, University of Chinese Academy of Sciences, Beijing 100049, China*

† Electronic supplementary information (ESI) available. See DOI: 10.1039/c8sm01871e

its motion. Therefore, the precise microscopic mechanisms of the phototaxis of artificial Janus microswimmers still remains to be elucidated.

In this paper, we perform mesoscale simulations to study the phototaxis of a self-thermophoretic Janus particle under both uniform and nonuniform beams. In both cases, the active Janus particle is found to have positive or negative phototaxis, depending on the particle–solvent interactions. Particularly, the particle alignment does not always coincide with its phototactic motion, in contrast to the interpretations in previous work. Our results indicate that the phototaxis of the active Janus particle originates from competition between three different factors, including the alignment effect, the orientation-dependent motility and the position-dependent motility. The rest of the paper is organized as follows. The simulation model and method are outlined in Section II, simulation results and discussion are presented in Section III, and a brief summary is provided in Section IV.

II. Simulation model and method

For simplicity, we consider a 2D active colloidal system. In most experiments phototactic active particles usually exhibit 2D motions near the substrate due to hydrodynamic interactions or sedimentation.[16,17,19,20] We use a hybrid mesoscale simulation scheme to bridge the drastic gap in both time and length scales between the solvent molecules and the colloidal particle. Here, a particle-based mesoscopic method known as multi-particle collision dynamics (MPC)[24–28] is used for the solvent, while the Janus particle and its interactions with the solvent are described by standard molecular dynamics (MD).

A. MPC fluid

In MPC, the solvent is modelled as a large number N of point-like particles of mass m with continuous positions $\mathbf{r}_i(t)$ and velocities $\mathbf{v}_i(t)$. The algorithm consists of alternating streaming and collision steps. In the streaming step, all the solvent particles move ballistically for a time h. In the collision step, particles are sorted into a square lattice with lattice size a, and interchange momentum relative to the center-of-mass velocity of each collision cell. In our simulations the stochastic rotation collision rule with variable collision angle α introduced by Ryder and Yeomans[27,29] is employed. This collision rule locally conserves mass, linear momentum, energy and angular momentum. It can therefore be proved that the algorithm properly captures hydrodynamic interactions, thermal fluctuations, thermal conduction and dissipation. Simulation units are reduced by setting $a = 1$, $m = 1$, and the system mean temperature $k_B\bar{T} = 0.5$ with k_B the Boltzmann constant. From the basic MPC units, the time unit is $a\sqrt{m/k_BT}$. We employ MPC parameters $h = 0.1$ and the mean number of solvent particles per cell $\rho = 30$. From the kinetic theory of MPC with a fixed rotation angle $\alpha = 90°$,[30] we can approximately calculate the Schmidt number as $Sc \simeq 33$, which corresponds to liquid-like dynamics.

B. Self-thermophoretic Janus particle

The Janus particle is modelled as a single bead with a defined body-fixed orientation vector $\mathbf{n}$ (symmetric axis), whose two hemispheres (2D) have different physical properties. Without loss of generality, the forward hemisphere (with the polar angle $\theta \leq \pi/2$ with respect to $\mathbf{n}$, see Fig. 1(a)) is prescribed to model the light-absorbing material and it can heat the surrounding fluid in a beam and create a local thermal gradient. As the two hemispheres of the Janus particle are material-heterogeneous, their interactions with the solvent are usually different. To mimic this, we employ a polar angle-dependent potential to describe the coupling between the Janus particle and the solvent,

$$U(r,\theta) = [1 + \delta\cos(\theta + \theta_0)] \times \tilde{U}(r)$$
$$\tilde{U}(r) = 4\varepsilon\left[\left(\frac{\sigma}{r}\right)^{2n} - \left(\frac{\sigma}{r}\right)^{n}\right] + c \quad r \leq r_c. \tag{1}$$

Here, r refers to the distance from the bead center to the solvent particle, and the polar angle θ is taken in the reference frame of the Janus particle. The radial potential $\tilde{U}(r)$ is a Lennard-Jones (LJ) type potential,[28] where ε is the potential intensity, σ is the bead radius, n is a positive integer describing the potential stiffness and r_c is the cutoff distance. The angular potential accounts for the anisotropic particle–solvent interactions, with $0 \leq \delta < 1$ describing the degree of anisotropy. Moreover, in order to properly model the rotational diffusion of the Janus particle, a sticky boundary condition is implemented on the particle surface through a revised bounce-back collision rule.[31]

In the self-generated temperature gradient around the heated hemisphere, the Janus particle exhibits self-thermophoretic motion. Thermophilic or thermophobic motion can be achieved using repulsive or attractive potentials, respectively.[32] An intuitive

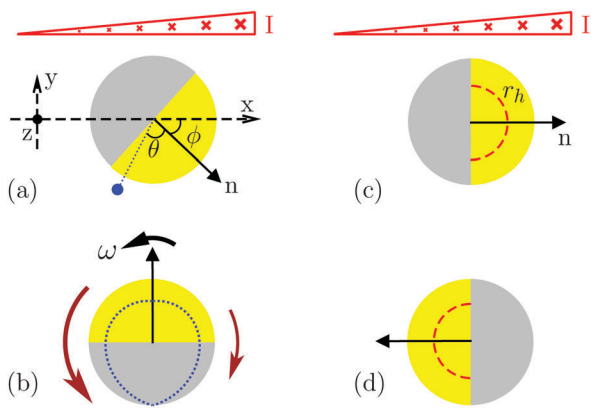

Fig. 1 (a) Schematic diagram of the self-thermophoretic active Janus particle in the light gradient. Here, the beam is applied against the z axis with its intensity gradient in the x direction, and the Janus particle, whose yellow hemisphere absorbs the light and heats the solvent, moves in the xy plane. (b) Rotation of the Janus particle induced by the asymmetric tangential forces (red arrows) on the particle. Here, the blue dashed line sketches the colloid–solvent angular potential. (c and d) Orientation-dependent motility of the Janus particle arising from the inhomogeneous beam and the non-vanishing size of the particle. The red dashed line refers to the light-sensing radius, r_h, at which the light energy flux is taken for heating the fluid around the yellow hemisphere.

picture for the propulsion mechanism can be drawn as follows. The MPC solvent has an ideal gas equation of state, so the solvent density is lower around the heated hemisphere than the non-heated one. The larger number of particles on the non-heated side produce stronger interactions. Consequently, the repulsive colloid–solvent interactions push the Janus particle towards high temperatures, namely self-propelling along the axis n; whereas the Janus particle with attractive interactions self-propels against the axis n. Besides, the angular potential introduces a nonuniform tangential coupling between the particle and solvent. Since the self-generated thermal gradient is usually asymmetrically distributed with respect to the axis n, the Janus particle can be subject to nonsymmetric tangential forces. This translates into a thermophoretic torque on the Janus particle and hence a rotation. For the repulsive potential, we take $c = \varepsilon$, $\varepsilon = 1$ and $\theta_0 = \pi$; while for the attractive case, we take $c = 0$, $\varepsilon = 1/4$ and $\theta_0 = 0$. With such choices, the thermophilic and thermophobic Janus particles have a similar self-propelled speed under the same light intensity. In the simulations, the radius of the Janus particle is set $\sigma = 5$. The equations of motion of the Janus particle and its neighbouring solvent are integrated by the velocity-Verlet algorithm with a time step $\Delta t = h/50$. The hybrid mesoscale simulations are performed with home-made code.

C. Light field and thermostat

We investigate the phototaxis of the Janus particle in two different light fields: an inhomogeneous beam with a constant intensity gradient as sketched in Fig. 1 and a uniform beam as sketched in Fig. 2. In the first case, we only consider the phototactic motion of the Janus particle in the gradient direction, and disregard its motion in the beam direction. This corresponds to the experiment of Lozano *et al.*,[16] in which a Janus particle stays on the substrate and performs 2D self-diffusiophoretic motion under an inhomogeneous beam normal to the substrate. In the second case, we study the phototactic motion of the Janus particle in the beam direction induced due to the shading effect, which corresponds to the experiment by Dai *et al.*[15]

In the simulations, we do not explicitly model the light field and its interactions with the particle, but only consider its heating effect. Concretely, the light is modelled as an energy flux, which is position-dependent for the inhomogeneous beam and is constant for the uniform beam. The simulation box is a rectangle of dimensions $L_x \times L_y = 120 \times 60$. To avoid the effect of the boundary wall on the phototaxis, which can cause an extra accumulation of active particles,[33] we use periodic boundary conditions (PBC) in both directions. The nonuniform beam is applied against the z direction and its energy flux changes linearly along the x direction (see Fig. 1), $I(x) = 0.02x$ for $x \leq L_x/2$, with a maximum in the middle of the system, such that it has a symmetric profile with respect to $x = L_x/2$, while the uniform beam with constant I is applied along the x axis (see Fig. 2).

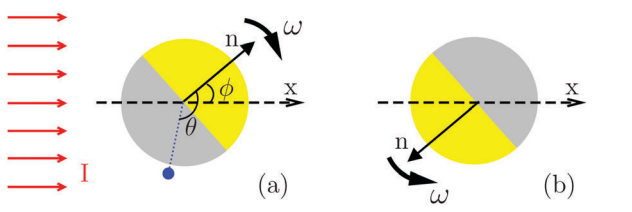

Fig. 2 Schematic diagram of the self-thermophoretic Janus particle in the uniform beam, which is applied along the x axis. (a and b) Alignment and orientation-dependent motility of the Janus particle, which are both induced due to the shading effect.

The light-heating effect is modelled by using local thermostats on the particle surface to heat the surrounding solvent.[31,32,34] Specifically, a thin layer of fluid around the heated (light-absorbing) hemisphere of the Janus particle is divided into small elements. For each element, a small amount of energy is added to thermal kinetic energy of the solvent particles inside by rescaling their velocities relative to the center-of-mass velocity of the element. The input energy depends on the coordinates of the element and the prescribed energy flux. For the nonuniform beam, the energy flux for heating the fluid element is taken as $I(x_c + r_h \cos(\phi + \theta))$ with x_c the x-coordinate of the Janus particle center and θ the polar angle of the fluid element. Here, we introduce a light-sensing radius r_h of the Janus particle (Fig. 1(c)), which characterizes the light-absorbing interface of the Janus particle. For experiments, r_h is just the particle radius. In simulations, however, r_h is an adjustable parameter ($\sigma \geq r_h \geq 0$), independent of the particle radius σ, that determines the angular dependence of the energy that goes into each surface element. Note that the thermostat operations for heating fluid molecules always occur at the particle surface instead of r_h. This tunable r_h thus allows us to systematically change the orientational dependence of the particle motility that originates from the fact that the colloidal particle has a finite size instead of being a point particle. For the uniform beam, the heated elements on the irradiated and shaded sides experience different light intensity. In order to mimic the shading effect and diffraction (the particle size is comparable to the optical wavelength), we simply require the light energy flux on the shaded side to be one-fourth of that on the irradiated side in the simulations. This difference in light energy flux between the shady and irradiated sides is similar to the one for a uniform beam diffracted by a disk with its radius equal to the optical wavelength. In this uniform case, the light-sensing radius r_h does not play a role.

The simple local thermostat neglects heat transfer from the colloidal particle to the fluid, as the colloidal particle lacks internal degrees of freedom. However, outside the heating layer, the energy is locally conserved such that the heat conduction process is physically correct. The resulting temperature field is consistent with the heat diffusion equation, as has been verified in previous work.[32] This thermostat locally conserves momentum such that hydrodynamic behaviors are not influenced. The input energy is drained from the system by fixing the mean temperature of the solution, $\bar{T}$, to a lower value, which is realized by uniformly rescaling the velocities of all the fluid particles relative to the solvent center-of-mass velocity. Since the system is large, this operation hardly affects the particle dynamics.

In our simulations, the colloidal particles are considered to be of low thermal conductivity, so the fluid temperature around the Janus particle is highly inhomogeneous. It is expected that

an active particle of high thermal conductivity will produce a relatively small temperature gradient and hence weak self-thermophoresis.

III. Results and discussion

Intuitively, besides the particle alignment induced by the anisotropic particle–fluid interaction, the orientation-dependent motility, resulting from the orientation-dependent optical absorption, may also give rise to phototaxis of the Janus particle. This effect exists even for an isotropic interaction. In addition, the nonuniform beam can generate a spatially varying motility that could also contribute to the phototaxis. To identify the possible mechanisms and disentangle their contributions, we systematically change the anisotropic parameter δ in the simulations so that the alignment can be gradually tuned. Furthermore, we tune the light-sensing radius r_h so as to change the orientational dependence of the motility. Particularly, when $r_h = 0$, the motility is independent of the particle orientation, although the heating performed on the particle surface still creates a local thermal gradient to drive self-thermophoretic motion. In this case, the Janus particle behaves like an active Brownian particle with position-dependent motility, which allows us to investigate the effect of the inhomogeneous motility exclusively.

A. Phototaxis in an inhomogeneous beam

To study the alignment effect, we first consider a thermophilic Janus particle (repulsive $\tilde{U}(r)$) with a relatively strong angular potential, $\delta = 0.5$, which is expected to produce a significant alignment of the Janus particle in the light gradient. As plotted in Fig. 3(a), the steady-state distribution of the particle orientation, ϕ (the included angle between the **n** and x axes), possesses a prominent maximum at π, namely pointing against the x direction. The alignment results from the difference in the tangential forces on the two sides of the Janus particle with respect to **n** due to the inhomogeneous illumination, as is intuitively illustrated in Fig. 1(b). Firstly, the angular potential has a maximum at $\theta = \pi$ and a minimum at $\theta = 0$, such that the tangential force exerted on the Janus particle is along the polar angle θ. Secondly, the light gradient generates a higher temperature, and hence lower density and smaller tangential force, on the right side of the Janus particle than on the left side. Thus, the Janus particle suffers from a counter-clockwise torque and rotates to the negative x-direction (*i.e.* **n** antiparallel to the x axis). At the same time, the self-generated local thermal gradient drives the thermophilic particle to self-propel towards the coated (heating) end. As a consequence, the active particle accumulates in the area of low beam intensity around $x = 0$ (we only consider the left half of the simulation box owing to symmetry), and exhibits negative phototaxis (Fig. 3(b)). This scenario is consistent with the previous experimental findings on self-diffusiophoretic Janus particles.[16]

As the anisotropic degree δ decreases, the tangential force on the particle and hence the alignment effect weaken, as plotted in Fig. 3(a). However, even in the case of isotropic potential $\delta = 0$, the polarization ($\phi = \pi$) does not disappear yet, suggesting that there are other mechanisms to orient the Janus particle. The residual polarization comes from the fact that the enhanced temperature around the Janus particle depends on its orientation (see Fig. 1(c and d)). With the local equilibrium assumption, the rotational degree of freedom of the particle basically obeys an ideal gas-like equation of state, such that the particle most likely points against the light gradient where the enhanced temperature is minimum. Surprisingly, the phototaxis of the active particle changes the sign from negative to positive with reducing δ (Fig. 3(b)), apparently inconsistent with the particle polarization. This implies that the alignment is not the only factor for the phototaxis, in contrast to the argument in previous work.[15,16] The positive phototactic behavior can be understood by noting that the orientation-dependent heating leads to an orientation-dependent motility with its maximum and minimum respectively at $\phi = 0$ and π for the same particle position (Fig. 1(c and d)). Thus, the orientation-dependent motility that exists for any δ drives the thermophilic Janus particle to averagely move to the high intensity region. For the present model, the alignment and the orientation-dependent motility compete with one another. At large δ, the alignment dominates and the active particle displays negative phototaxis, otherwise the active particle behaves phototactically.

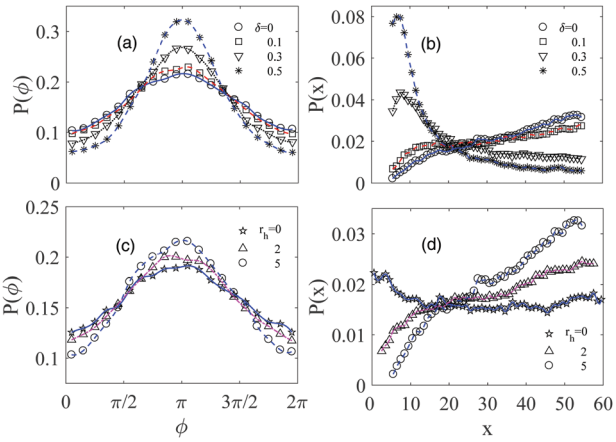

Fig. 3 Orientation probability distribution $P(\phi)$ and position probability distribution $P(x)$ of the thermophilic active Janus particle in the inhomogeneous light field. (a) $P(\phi)$ and (b) $P(x)$ for various δ with $r_h = 5$ fixed. (c) $P(\phi)$ and (d) $P(x)$ for different r_h with $\delta = 0$ fixed.

The orientational dependence of the heating weakens with diminishing the light-sensing radius r_h of the particle (Fig. 1(c and d)). Thus, for an isotropic potential of $\delta = 0$ both the alignment effect and the orientational dependence of the motility reduce as r_h decreases, as displayed in Fig. 3(c and d). At $r_h = 0$ the heating is independent of the orientation such that the motility is isotropic, but the polarization does not completely vanish and the Janus particle becomes negatively phototactic again. This remarkable behavior means that there exists a third mechanism responsible for the alignment and phototaxis. To understand this, we notice that for $\delta = 0$ and $r_h = 0$, the nonuniform beam mainly generates an x-dependent self-propelled velocity, $v_s(x)$. In this case, the Janus particle

may be approximated as an active Brownian particle with spatially inhomogeneous motility, neglecting hydrodynamics and thermal conduction. For simplicity, the diffusion coefficient and temperature are considered to be constant. Thus, the active Janus particle can be described through overdamped Langevin equations, $\dot{\mathbf{r}} = v_s(x)\mathbf{n} + \sqrt{2D_t}\xi$ and $\dot{\phi} = \sqrt{2D_r}\zeta$, where ξ and ζ are zero-mean unit-variance Gaussian white noise, and D_t and D_r are the translational and rotational diffusion coefficients, respectively.

The Smoluchowski equation for the probability distribution, $\Psi(\mathbf{r},\phi,t)$, can be constructed from the Langevin equations as[35–38]

$$\partial_t\Psi + \nabla\cdot[v_s(x)\mathbf{n}\Psi] - D_t\nabla^2\Psi - D_r\partial_\phi{}^2\Psi = 0. \quad (2)$$

Integrating eqn (2) over ϕ, we can obtain an equation for the density, $\rho(\mathbf{r}) = \int\Psi \mathrm{d}\phi$, in the steady state as

$$v_s(x)\mathcal{P} - D_t\partial_x\rho(x) = 0. \quad (3)$$

Here, $\mathcal{P} = \int\Psi\cos(\phi)\mathrm{d}\phi$ is the polarization field, and vanishing particle current has been used due to the system symmetry. By translational invariance, ρ and $\mathcal{P}$ are only functions of x. Multiplying eqn (2) by $\cos\phi$ and integrating over ϕ, we can obtain a steady-state equation for $\mathcal{P}$ as

$$\mathcal{P} \simeq -\frac{1}{2D_r}\partial_x[v_s(x)\rho(x)], \quad (4)$$

in which higher order terms have been neglected. Combining eqn (3) and (4) yields

$$\frac{v_s(x)}{2D_r}\partial_x[v_s(x)\rho(x)] + D_t\partial_x\rho(x) = 0. \quad (5)$$

For large Péclet number $\mathrm{Pe} = v_s\sigma/D_t$ (convective transport dominates), eqn (5) implies $\rho(x) \sim 1/v_s(x)$. This indicates that the active particle of $r_h = 0$ accumulates in areas with low motility and hence is negatively phototactic, which explains the simulation result in Fig. 3(d). Furthermore, from eqn (3) we have $\mathcal{P} \sim \partial_x\rho(x)$ such that the thermophilic Janus particle aligns its orientation along the density gradient, namely against the light intensity gradient, consistent with the simulation result in Fig. 3(c). These results about the active Brownian particle are also in agreement with previous theoretical work.[35,39]

To exclusively study the proposed theoretical model of inhomogeneous motility and to avoid the possible effect of position-dependent local heating, we perform a pure Brownian dynamics simulation with spatially varying $v_s(x)$ (Fig. 4(b)) and constant T, D_t and D_r. Here, $v_s(x)$ is chosen according to the above fluid simulation, and T, D_t and D_r are separately taken as the mean temperature and diffusion coefficients in the fluid simulation. The particle density distribution in Fig. 4(b) decreases with increasing v_s, namely negative phototaxis. However, $\rho(x)v_s(x)$ quickly increases and saturates to a constant at a moderate v_s, above which convective transport is dominant. At small v_s, the diffusive term in eqn (5) cannot be ignored, which translates into the orientation of the active particle against the x axis, as shown in Fig. 4(a). These unambiguously confirm that inhomogeneous motility can also lead to the phototaxis and alignment of the active Janus particle.

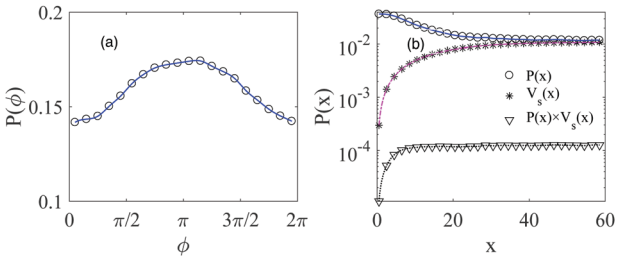

Fig. 4 (a) Orientation probability distribution and (b) position probability distribution of the active Brownian particle with spatially varying motility. Here, the system parameters are taken according to the thermophilic Janus particle of $\delta = 0$ and $r_h = 0$. In (b) the self-propelled velocity, $v_s(x)$, and $P(x)v_s(x)$ are also plotted.

The phototaxis of the active Janus particle has been quantified by the stationary positional and orientational distributions. In order to look into the dynamics of the phototactic particle, we also measure the orientation- and position-dependent angular velocities and self-propelled velocities of the Janus particle, which are presented in the ESI.† Moreover, we investigate the finite-size effect on the fluid simulations due to particle self-interactions *via* periodic boundary conditions (see also the ESI†), which shows that the finite-size effect only slightly influences the obtained results.

Based on the thermophilic colloid, we have already identified three different mechanisms for the phototaxis of the active Janus particle by independently tuning the interaction anisotropy and light-sensing radius. For comparison, we also study the phototactic motion of a thermophobic active Janus particle that can be easily realized in the simulation using attractive $\tilde{U}(r)$.[31,32] Similar to the thermophilic case, a large δ can generate a strong thermophoretic torque that aligns the Janus particle against the light gradient, as shown in Fig. 5(a). It is predicted to lead to positive phototaxis, since the self-propelled velocity of the thermophobic particle is antiparallel to $\mathbf{n}$. However, Fig. 5(b) shows a contradictory trend, *i.e.* negative phototaxis. The reason for the contradiction is that the orientation-dependent motility that contributes to negative phototaxis overwhelms the alignment effect. This demonstrates again that the phototaxis of the active particle is not solely determined by its alignment. At $\delta = 0$, the alignment due to the thermophoretic torque vanishes, but a relatively weaker polarization of the Janus particle from the orientation-dependent heating ($r_h \neq 0$) still exists, as shown in Fig. 5(a). As a consequence, the negative phototaxis becomes stronger than in the case of anisotropic

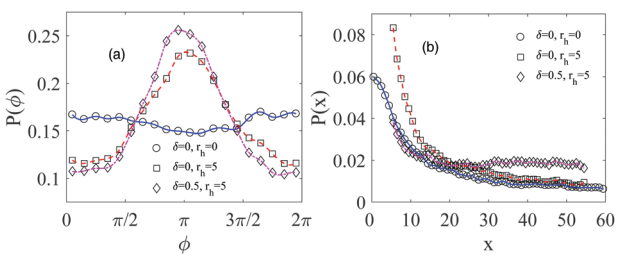

Fig. 5 Orientation and position probability distribution of the thermophobic active Janus particle in the inhomogeneous light field. (a) $P(\phi)$ and (b) $P(x)$ for various δ and r_h.

potential (Fig. 5(b)). Finally, for $\delta = 0$ and $r_h = 0$ the orientation-dependent heating-induced polarization and phototaxis are lacking, such that the active Janus particle roughly reduces to the active Brownian particle with an inhomogeneous self-propelled velocity. In terms of eqn (2)–(5), the phototactic behavior is always negative and the active particle orients in such a way that it moves toward the region of low beam intensity, which agrees with the results in Fig. 5. All these findings can thus be well explained in terms of the competition of the three proposed mechanisms above.

B. Phototaxis in a uniform beam

In this section, we investigate the phototactic motion of the active Janus particle in a uniform beam (see Fig. 2). In this situation, the light intensities experienced by the particle on its irradiated and shaded sides are different due to the shading effect, which breaks the fore-and-aft symmetry in the beam direction and hence biases the motion of the Janus particle.

By the same analysis as the case of the inhomogeneous beam, for $\delta \neq 0$ the thermophoretic torque rotates the Janus particle until its absorbing cap is against the light source, namely $\phi = 0$ in Fig. 2. Because the thermophoretic torque is an increasing function of δ and the light energy flux, the alignment effect diminishes with the decrease of δ and I, as plotted in Fig. 6(a–d). Nevertheless, for an isotropic potential and nonzero I, the particle alignment vanishes. This seems inconsistent with the orientation-dependent heating-induced polarization that is expected to be against the light source, as discussed in Section IIIA. The reason for the inconsistency is that thermal creep[40,41] occurring at the nonslip particle surface heated asymmetrically may produce a small opposite torque.[42] Thermal creep is an effect in rarified gases and cannot be completely avoided in the coarse-grained fluid simulations.[43]

In the uniform beam, the motility is independent of the particle position in contrast to the case of the inhomogeneous beam. As such, the phototaxis of the Janus particle only arises from the alignment effect and the orientation-dependent motility.

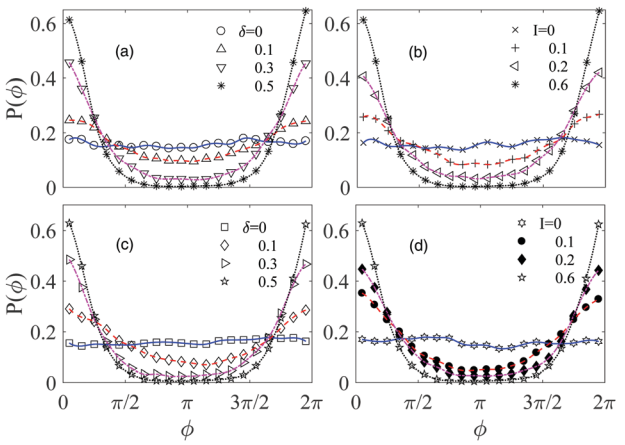

Fig. 6 Orientation probability distribution of the active Janus particle in the homogeneous beam. (a) Thermophilic and (c) thermophobic Janus particles for various δ with $I = 0.6$ fixed; (b) thermophilic and (d) thermophobic Janus particles for various I with $\delta = 0.5$ fixed.

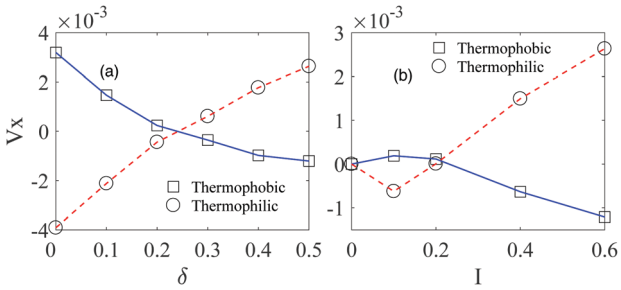

Fig. 7 The x-component of the mean drift velocity of the active Janus particle in the homogeneous beam as a function of δ with $I = 0.6$ (a), and as a function of I with $\delta = 0.5$ fixed (b). Here, circles and squares correspond to the thermophilic and thermophobic Janus particles, respectively.

Since the periodic boundary condition is imposed in the beam direction, the phototactic behavior of the Janus particle is reflected by its drift velocity along the x axis relative to the light source instead of its (uniform) probability distribution. For high δ and I, the alignment effect is strong and dominates the phototactic motion of the particle. In this case (polarization at $\phi = 0$), the thermophobic and thermophilic active particles move toward (positive phototaxis) and away from (negative phototaxis) the light source, respectively, as shown in Fig. 7. However, for weak polarization, the orientation-dependent motility determines the phototaxis. Since the particle motility is maximum at $\phi = \pi$ (the light-absorbing cap is on the irradiated side), the thermophobic and thermophilic Janus particles exhibit respectively negative and positive phototaxis, in agreement with the results in Fig. 7. As a result of the competition between these two mechanisms, the phototactic motion of the active Janus particle changes direction with δ and I. Clearly, at $I = 0$ the Janus particle becomes passive and hence the phototaxis disappears. Thus, the phototactic behavior of the active Janus particle in the uniform beam can also be understood on the basis of the proposed mechanisms.

For the homogeneous beam, the angular and self-propelled velocities of the phototactic Janus particle and the finite-size effect on the simulations are also presented in the ESI.†

IV. Conclusions

In this paper, we perform mesoscale dynamics simulations to study the phototactic behavior of an active Janus particle driven by self-thermophoresis due to optical heating. We show that the artificial microswimmer can sense and orient to the intensity gradient of inhomogeneous light and the illumination direction of a uniform beam. Both positive and negative phototaxis can be achieved, depending on the interactions between the active particle and fluid. We find that the phototaxis of the active colloid arises from the competition of three different mechanisms, including the particle alignment, the orientation-dependent motility and the spatially varying motility. This highlights that the phototaxis of the active Janus particle cannot be solely determined by its polarization. These findings provide deeper insight into phototaxis of synthetic active colloids and are

of importance for understanding the related experimental phenomena.

Because external light fields can be flexibly and remotely regulated, phototaxis offers an ideal way to manipulate active colloids in a complex environment. Unlike existing studies on phototaxis in which artificial active colloids are powered by light-induced chemical gradients, the present work takes advantage of self-thermophoresis induced by optical heating. Such thermal gradient-driven microswimmers are fuel-free and respond quickly, so phototaxis based on self-thermophoresis is expected to be more promising for control of active particles.

Conflicts of interest

There are no conflicts to declare.

Acknowledgements

We thank Alois Würger for useful discussions. We acknowledge support from the National Natural Science Foundation of China (Grant No. 11874397, 11674365, 11474327). This work was also supported by the MOST 973 Program (No. 2015CB856800).

References

1 W. Nultsch, H. Schuchart and M. Höhl, *Arch. Microbiol.*, 1979, **122**, 85.
2 A. Giometto, F. Altermatt, A. Maritan, R. Stocker and A. Rinaldo, *Proc. Natl. Acad. Sci. U. S. A.*, 2015, **112**, 7045.
3 W. F. Paxton, K. C. Kistler, C. C. Olmeda, A. Sen, S. K. S. Angelo, Y. Cao, T. E. Mallouk, P. E. Lammert and V. H. Crespi, *J. Am. Chem. Soc.*, 2004, **126**, 13424.
4 J. R. Howse, R. A. L. Jones, A. J. Ryan, T. Gough, R. Vafabakhsh and R. Golestanian, *Phys. Rev. Lett.*, 2007, **99**, 048102.
5 H. R. Jiang, N. Yoshinaga and M. Sano, *Phys. Rev. Lett.*, 2010, **105**, 268302.
6 J. Palacci, C. Cottin-Bizonne, C. Ybert and L. Bocquet, *Phys. Rev. Lett.*, 2010, **105**, 088304.
7 J. Palacci, S. Sacanna, A. P. Steinberg, D. J. Pine and P. M. Chaikin, *Science*, 2013, **339**, 936.
8 I. Buttinoni, J. Bialké, F. Kümmel, H. Löwen, C. Bechinger and T. Speck, *Phys. Rev. Lett.*, 2013, **110**, 238301.
9 Y. Hong, N. M. Blackman, N. D. Kopp, A. Sen and D. Velegol, *Phys. Rev. Lett.*, 2007, **99**, 178103.
10 L. Baraban, S. M. Harazim, S. Sanchez and O. G. Schmidt, *Angew. Chem., Int. Ed.*, 2013, **52**, 5552.
11 E. Paster and W. S. Ryu, *Proc. Natl. Acad. Sci. U. S. A.*, 2008, **105**, 5373.
12 T. Bickel, G. Zecua and A. Würger, *Phys. Rev. E: Stat., Nonlinear, Soft Matter Phys.*, 2014, **89**, 050303.
13 B. T. Hagen, F. Kümmel, R. Wittkowski, D. Takagi, H. Löwen and C. Bechinger, *Nat. Commun.*, 2014, **5**, 4829.
14 J. Palacci, S. Sacanna, A. Abramian, J. Barral, K. Hanson, A. Grosberg, D. Pine and P. Chaikin, *Sci. Adv.*, 2015, **1**, e1400214.
15 B. Dai, J. Wang, Z. Xiong, X. Zhan, W. Dai, C. C. Li, S. P. Feng and J. Tang, *Nat. Nanotechnol.*, 2016, **11**, 1087.
16 C. Lozano, B. T. Hagen, H. Löwen and C. Bechinger, *Nat. Commun.*, 2016, **7**, 12828.
17 C. Chen, F. Mou and L. Xu, *et al.*, *Adv. Mater.*, 2017, **29**, 1603374.
18 W. Li, X. Wu, H. Qin, Z. Zhao and H. Liu, *Adv. Funct. Mater.*, 2016, **26**, 3164.
19 Z. Ye, Y. Sun, H. Zhang, B. Song and B. Dong, *Nanoscale*, 2017, **9**, 18516.
20 Z. Lin, T. Si, Z. Wu, C. Gao, X. Lin and Q. He, *Angew. Chem.*, 2017, **56**, 13517.
21 A. P. Bregulla, H. Yang and F. Cichos, *ACS Nano*, 2014, **8**, 6542.
22 M. Xuan, Z. Wu, J. Shao, L. Dai, T. Si and Q. He, *J. Am. Chem. Soc.*, 2016, **138**, 6492.
23 J. A. Cohen and R. Golestanian, *Phys. Rev. Lett.*, 2014, **112**, 068302.
24 A. Malevanets and R. Kapral, *J. Chem. Phys.*, 1999, **110**, 8605.
25 J. T. Padding and A. A. Louis, *Phys. Rev. E: Stat., Nonlinear, Soft Matter Phys.*, 2006, **74**, 031402.
26 R. Kapral, *Adv. Chem. Phys.*, 2008, **140**, 89.
27 G. Gompper, T. Ihle, D. M. Kroll and R. G. Winkler, *Adv. Polym. Sci.*, 2009, **221**, 1.
28 D. Lüsebrink, M. Yang and M. Ripoll, *J. Phys.: Condens. Matter*, 2012, **24**, 284132.
29 J. F. Ryder, *Mesoscopic Simulations of Complex Fluids*, PhD thesis, University of Oxford, 2005.
30 E. Tüzel, T. Ihle and D. M. Kroll, *Phys. Rev. E: Stat., Nonlinear, Soft Matter Phys.*, 2006, **74**, 056702.
31 M. Yang, A. Wysocki and M. Ripoll, *Soft Matter*, 2014, **10**, 6208.
32 M. Yang and M. Ripoll, *Phys. Rev. E: Stat., Nonlinear, Soft Matter Phys.*, 2011, **84**, 061401.
33 J. Elgeti and G. Gompper, *EPL*, 2013, **101**, 48003.
34 X. Lou, N. Yu, R. Liu, K. Chen and M. Yang, *Soft Matter*, 2018, **14**, 1319.
35 M. E. Cates and J. Tailleur, *Europhys. Lett.*, 2013, **101**, 20010.
36 J. Bialké, H. Löwen and T. Speck, *Europhys. Lett.*, 2013, **103**, 30008.
37 R. Golestanian, *Phys. Rev. Lett.*, 2012, **108**, 038303.
38 M. Hennes, K. Wolff and H. Stark, *Phys. Rev. Lett.*, 2014, **112**, 238104.
39 S. Saha, R. Golestanian and S. Ramaswamy, *Phys. Rev. E: Stat., Nonlinear, Soft Matter Phys.*, 2014, **89**, 062316.
40 J. C. Maxwell, *Philos. Trans. R. Soc. London*, 1879, **170**, 231.
41 Y. Sone, *Annu. Rev. Fluid Mech.*, 2000, **32**, 779.
42 We implemented an independent simulation of the active Janus particle of $\delta = 0$ in the uniform beam. Here, the particle position and orientaion are fixed with $\phi = \pi/2$. The particle indeed experiences a small positive torque, which tends to rotate the particle anticlockwise, namely toward the light source.
43 M. Yang and M. Ripoll, *Soft Matter*, 2013, **9**, 4661.

